A Multi-Input DC-DC Converter for an Energy Management System in Electric Vehicles

Rahul Nair K[1], Raj Kumar G[2]

[1]Student, Department of Electrical and Electronics Engineering, Nehru College of Engineering and Research Centre, Kerala, India

[2]Asst. Professor, Department of Electrical and Electronics Engineering, Nehru College of Engineering and Research Centre, Kerala, India

---***---

Abstract- *In order to process the electrical power in hybrid energy storage systems (HESSs), this paper proposes a novel bidirectional non-isolated multi-input converter (MIC) topology for an energy management system (EMS) in electric vehicles. It has different electrical characteristics to transfer power from different input voltage sources to the output. The proposed converter has the ability of controlling the electrical power of HESSs by allowing active power sharing. The voltage levels of utilized HESSs can be greater or lesser than the output voltage. The inductors of the converter are connected to a switch. Therefore, the converter requires only one extra active switch for each input, hence results in the reduced part count. The proposed MIC topology is compared with its equivalent converters concerning various parameters. It is studied in detail, then this analysis is validated by simulation and a 255W prototype based on a battery/ultra-capacitor (UC) hybrid ESS.*

Key Words: **Batteries, energy management system, hybrid energy storage systems, ultra-capacitor, multi-input converter**

I. INTRODUCTION

There are lots of researches conducted on hybrid electric vehicles (HEVs), electric vehicles (EVs), and plug-in hybrid electric vehicles (PHEVs) due to the environmental and economic concerns [4], [1] in which hybrid energy storage systems (HESSs) have been inclusively studied. The motive of a HESS is to make use of drastic features of ESS elements while eliminating their deficiencies to achieve the potential of an ideal ESS element. In order to create a HESS having the characteristics of an ideal energy storage unit such as high energy/power density, low cost/weight per unit capacity, and long cycle life, researchers have hybridized batteries and UCs in [3].

The active hybridization of the aforementioned ESSs, in which the power/current can be controlled fully, by means of utilizing power converters. Power converter topologies used in HESS can be broadly classified into two main categories, i.e., isolated and non-isolated. In [8] isolated HESS topology includes a transformer in order to provide galvanic isolation between sources and output. Non-isolated power converters are unsophisticated in terms of design and control when compared to isolated ones. One of the easiest way to build a non-isolated HESS is to connect some of the sources directly while linking others to dc bus through a bidirectional dc-dc converter as in [2]; however, this method does not allow to calibrate the dc bus voltage. Unlike the former topology, the multiple converter topology design permits managing the output voltage; however, it is an expensive approach as it requires multiple converters. In order to decrease the cost of multiple converter topologies, multi input converter (MIC) topologies are reported in the literature [5], [12].

In addition to the MIC topology, EMS have been proposed [2]. When it comes to EMSs for HESSs, several works have been studied in the literature. EMSs reported in [2], [3] present a productive but non-flexible solution to energy management problem. This method basically applies the defined control principles through given rules according to the operation modes of the utilized converter. In [6] model predictive control (MPC) concept was implemented for battery/UC HESSs. This concept has the ability to predict future events and act according to these predictions; however, it needs an internal model of the whole system. In [9] offline optimization techniques were implemented for EMS in hybrid systems; however, they are inappropriate for the real-time applications. In [12] the fuzzy logic controller (FLC) based EMSs are proposed. FLC offers the benefit that it does not require any mathematical model or a prior knowledge of the system. Therefore, it can be merely utilized in an EMS. In [7] a battery/UC HESS through a novel MIC topology for EVs is proposed. In this system, a rule-based EMS is implemented to limit the battery power during propulsion and charge UC

---

during regenerative braking.

II. THE ANALYSIS OF THE PROPOSED CONVERTER

A novel SEPIC-based multi-input bidirectional dc- dc converter is studied in this paper. It has two inputs as illustrated in Fig.1. As it can be seen, the converter has four power switches namely S_1, S_2, T_0 and Q_0 with internal diodes, two power diodes namely D1 and D2, two capacitors namely C_1 and C_2, three inductors namely L_1, L_2 and L_3 and an output capacitor C_0.
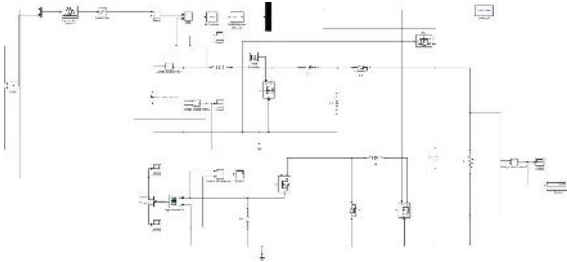

Fig.1. Proposed multi-input converter with two inputs

This MIC has mainly two operation modes. The first operation mode is called discharging mode. In this mode, the output is fed by input sources according to states of S_1, S_2 and Q_0. Power diodes D_1 and D_2 operate in compatible manner with S_1 and S_2, respectively. The second operation mode is called regenerative mode; in this mode, by controlling T_0, regenerative braking energy charges ESSs depending on their voltage levels. In regenerative mode, D_1 and D_2 are always OFF while the body diode of T_0 carries the inductor currents when Q_0 is OFF. These stages are applied effectively into the design of the SEPIC converter in order to achieve a feasible structure. It is important to note that the two input sources given in the MIC are ultra-capacitor and battery which are used in the ESS. It is convenient that the drawn ripple current from the input power sources is minimized. Therefore, the continuous conduction mode (CCM) and dynamic behavior of the proposed system are discussed in this study. Two main operation modes of the proposed converter are as follows:

A. Discharging mode ESS (First operation mode)

In this operation mode, the load power demand is high and the input power source (V_{in_1}) cannot supply the load by itself. Therefore, the ESS discharges to supply the load along with the input power source. The power switches S_1 and Q_0 are active in this operation mode while the switches S_2 and T_0 are inactive. The power

switch S_1 is accountable to control and regulate the inductor current (i_{L_1}) i.e. the output power of the V_{in_1}. The output voltage of the ESS is controlled through the power switch Q_0. The gate signals of the power switches, the voltage and current waveforms of the inductors are illustrated in Fig. 2. In this operation mode, three switching state will exist as follows.
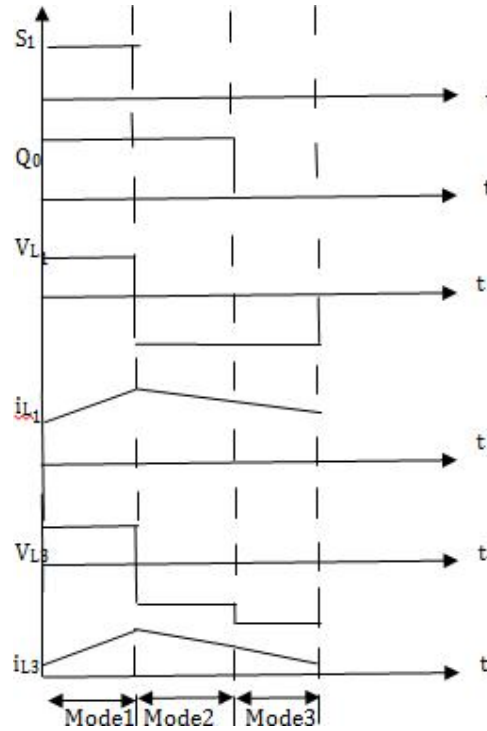

Fig: 2. Steady-state waveforms of the presented converter in the first operation mode.

Switching mode 1: The power switches S_1 and Q_0 are turned ON. The diode D_2 is reversely biased due to active switch Q_0. Also, the diode D_1 is reversely biased because the active switch S_1. In this switching mode, the input power source magnetizes the inductor L_1 and L_2. In addition, the inductor L_3 is magnetized by the ESS and the capacitor C_1. The ESS discharges through the inductor current i_{L_3}. The capacitor C_0 discharges to supply the load in this switching mode.

$$L_1 + \frac{di_{L_1}}{dt} = V_{in_1} \qquad \text{- (1)}$$

$$L_1 \frac{di_{L_1}}{dt} + L_3 \frac{di_{L_3}}{dt} = V_{ESS} + V_{C_1} \text{ - (2)}$$

$$C_1 \frac{dc_1}{dt} = -i \qquad \text{- (3)}$$

$$\frac{dV_{C_0}}{dt} = \frac{V_{C_0}}{R_L} \qquad \text{- (4)}$$

Switching mode 2: In this switching mode, the power switch S_1 is inactive while the switch Q_0 is still ON. The currents i_{L_1} and i_{L_3} force the diode D_1 to be active. Similar to the switching mode 1, the ESS discharges by the inductor current i_{L_3}. The inductors L_1, L_2 and L_3 demagnetizes by the voltages $V_{in_1} - V_{C_1} - V_{C_0}$ and $V_{ESS} - V_{C_0}$, respectively. The capacitors C_1 and C_0 are charged by the currents i_{L_1} and $i_{L_1} + i_{L_3}$, respectively.

$$L_1 \frac{di_{L_1}}{dt} = V_{in_1} - V_{C_1} - V_{C_0} \qquad - (5)$$

$$L_2 \frac{di_{L_2}}{dt} + L_3 \frac{di_{L_3}}{dt} = V_{ESS} - V_{C_0} \quad - (6)$$

$$C_1 \frac{dc_1}{dt} = i_{L_1} \qquad - (7)$$

$$\frac{dV_{C_0}}{dt} = i_{L_1} + i_{L_3} - \frac{V_{C_0}}{RL} \qquad - (8)$$

Switching mode 3 ($d_1 T_S < t < T_S$): In this switching mode, the switch Q_0 is inactive. Therefore, the ESS is not discharged. The inductors L_1 and L_2 are demagnetizes by the voltages $V_{in_1} - V_{C_1} - V_{C_0}$ and $-V_{C_0}$, respectively. Similar to the switching mode 2, the capacitors C_1 and C_0 are charged by the currents i_{L_1} and $i_{L_1} + i_{L_2}$, respectively. The following equations can be written in this switching mode:

$$L_1 \frac{di_{L_1}}{dt} = V_{in_1} - V_{C_1} - V_{C_0} \quad - (9)$$

$$L_2 \frac{di_{L_2}}{dt} = - V_{C_0} \qquad - (10)$$

$$C_1 \frac{dc_1}{dt} = i_{L_1} \qquad - (11)$$

$$\frac{dV_{C_0}}{dt} = i_{L_1} + i_{L_3} - \frac{V_{C_0}}{RL} \qquad - (12)$$

By applying the voltage-second balance equations for the inductors L_1 and L_2, the following equations can be deduced as follows:

$$V_{C_1} = V_{in_1} - (d_1)V_{ESS} \qquad - (13)$$

$$V_{C_0} = \frac{V_{in_1} i_{L_1} + (d_1)V_{ESS}}{1 - d_1} \qquad - (14)$$

The battery discharging power can also be derived by using the following equation:

$$V_0 = V_{bat} \frac{dS_1}{1 - dQ_0} \qquad - (15)$$

B. Charging mode ESS (Second operation mode)

In this operation mode, the input power source V_{in_2} supply the load and it also delivers the power in order to charge the ESS. This operation mode takes place when the load power demand is low or it is required to charge the ESS. In this operation mode, the

switches S_2 and T_0 are active. The power switch S_2 is responsible to control and regulate the inductor current i_{L_3}, i.e. the output power of the source V_{in_2}. The output voltage of the ESS is controlled through the power switch T_0. The gate signals of the power switches and the voltage and current waveforms of the inductors are illustrated in Fig. 3. In this operation mode, three switching state will exist as follows.

Switching mode 1: In this switching mode, the power switch S_2 is active. The diode D_2 is reversely biased when the switch S_2 is turned ON. The inductors L_3 and L_2 are charged by the input source V_{in_2} and V_{C_1}, respectively. The capacitor C_0 discharges to supply the load. The following equations can be derived in this switching mode:

$$L_3 \frac{di_{L_1}}{dt} = V_{in_2} \qquad - (16)$$

$$L_2 \frac{di_{L_2}}{dt} = V_{C_1} \qquad - (17)$$

$$C_1 \frac{dc_1}{dt} = - I \qquad - (18)$$

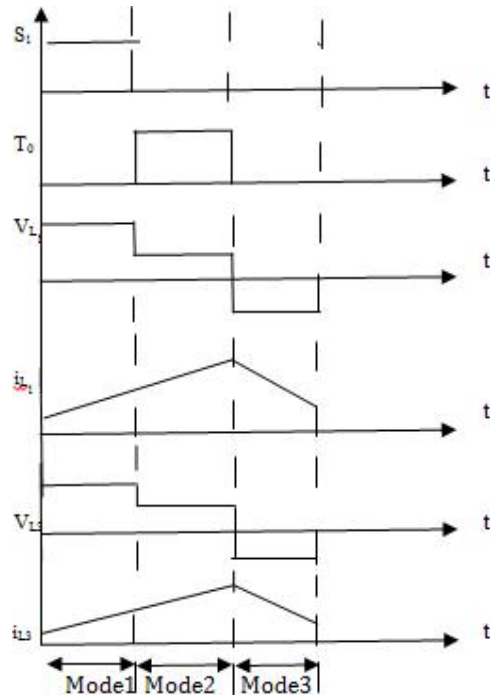$$\frac{dV_{C_0}}{dt} = \frac{V_{C_0}}{RL} \qquad - (19)$$

Fig. 3. Steady-state waveforms of the presented converter in the second operation mode.

Switching mode 2 ($d_1 T_S < t < (d_1 + d_2)T_S$): In this switching mode, the power switch S_2 is inactive while the power switch T_0 is active. The inductor

currents i_{L_1} and i_{L_3} flow through the switch T_0 to charge the ESS. As mentioned in the first switching mode, the capacitor C_0 supplies the load demand. The following equations can be written in this switching mode:

$$L_1 \frac{di_{L_1}}{dt} = V_{in_2} - VESS \qquad - (20)$$

$$L_3 \frac{di_{L_3}}{dt} = V_{C_1} - VESS \qquad - (21)$$

$$C_1 \frac{dV_{C_1}}{dt} = i_{L_3} \qquad - (22)$$

$$\frac{dV_{C_0}}{dt} = \frac{V_{C_0}}{RL} \qquad - (23)$$

Switching mode 3: This switching mode is similar to the third switching mode in the ESS discharging operation mode. By applying voltage-second balance equations for the inductors L_1 and L_2, the following equations can be deduced as follows:

$$V_{C_1} = V_{in_2} \qquad - (24)$$

$$V_{C_0} = \frac{(d_1 + d_2) V_{in_2} - d_2 VESS}{1 - d_1 - d_2} \qquad - (25)$$

The UC charging power can also be derived by using the following equation:

$$V_o = \frac{VUC}{dT_0} \qquad - (26)$$

This converter is able to operate even when input power sources are not available. This can be considered as an advantage for the proposed converter. In this case, the load power is supplied by the ESS.

II. A COMPARATIVE ANALYSIS OF CONVERTERS

In Table I, two topologies are compared Concerning various parameters. As can be seen from this table, consists of modified version of cascaded buck-boost converters (CBBC) branches that are connected in parallel. This topology enables buck operation as well during propulsion. Note that the modified CBBC is considered here for the sake of fair comparison in terms of active switch count. The proposed converter in this paper which is given in Fig. 1. has also buck/boost capability during propulsion with the advantage of fewer active switch requirement as stated in Table I. Table I also includes the switch stress analysis of examined converters. It is assumed that each input source equally shares the output

power in both directions.

TABLE I

COMPARISON OF BIDIRECTIONAL MULTI- INPUT CONVERTERS

Types of MIC			Modified CBBC Converter	Proposed Converter
Operation modes during propulsion/ regenerative braking			Buck-Boost/Buck	Buck-Boost/Buck
Number of switches			5	4
Switching stress during propulsi-on regenerat-ive breaking	S_1	Vol	V_0	V_0
		Cur	0.485	0.480
	S_2	Vol	V_0	V_0
		Cur	0.980	0.960
	T_0	Vol	V_0	V_0
		Cur	0.154	0.157
	Q_0	Vol	V_0	V_0
		Cur	0.603	0.603
	Q_1	Vol	V_0	-
		Cur	0.535	-

III. ENERGY MANAGEMENT SYSTEM

Fuzzy logic-based energy management strategy (FLEMS) determines the operation mode by checking the output voltage. If the output needs to be energized, the reference of battery power is determined by a FLC by taking the output voltage and SOC_{UC} into account. Here FLC determines the battery reference power so as to regulate SOC_{UC} at a reference value. This value should be regulated in a way that UC can supply the required load demand and has enough capacity to capture all the available braking energy. After this, a rate limiter restricts the slew rate of the battery power reference so as to smooth the battery power; and a proportional-integral (PI) controller adjusts the battery current to attain the desired battery power. In addition, the proposed control strategy chooses either discharging or charging modes by comparing the battery and output power levels: if the power of battery is lower than the output power, the discharging mode is activated; otherwise, the charging mode is activated. As studied in [2] although increasing d_{T0} expands the input voltage range of the converter, it also decreases the efficiency by increasing stresses on the switches. Therefore, d_{T0} is set to a rational value, i.e. 0.5 for discharging mode. Moreover, for regulating the dc bus and thus ultimately controlling the power of UC, d_{S2} and d_{T0} are controlled by PI controllers in the discharging mode and on the other hand, if an increase in the output voltage due to the existence of regenerative braking energy is sensed, the charging mode is activated. In the charging mode, another PI controller adjusts d_{Q0} for dc bus regulation. The explained mode selection procedure can be seen in Fig. 4 in which Δ is a defined voltage level. For designing PI controllers, the small signal model and design procedure presented in [5] are utilized in this study. It can be seen in several studies like [10], [12], FLC having

triangle membership functions perform well. FLC has two input membership functions: SOC_{UC} and Po. Finally, according to the rule base and defined membership functions, the reference of the battery power is calculated through the center-of-gravity defuzzification technique.

IF $V_o < V_o^* - \Delta$ and $P_{bat} < P_o$ **THEN**

Activate discharging mode.

ELSE IF $V_o < V_o^* - \Delta$ and $P_{bat} > P_o$ **THEN**

Activate charging/discharging mode.

ELSE IF $V_o > V_o^* + \Delta$ **THEN**

Activate regenerative mode.

END IF

Fig. 4. Mode selection procedure

V. SIMULATION AND EXPERIMENTAL RESULTS

In this study, an average model of the proposed converter is built in MATLAB/Simulink based on [11], [12]. Here, a Li-Ion battery with 110 Ah nominal capacity, 100 V nominal voltage and an UC with 63 F rated capacitance, 125 V rated voltage are considered. Battery and UC are modeled in the simulation through (27)-(29) and (30)-(32), respectively.

$$i_{bat}(t) = i_{L1}(t)d_{S1} \quad\text{- (27)}$$

$$v_{bat,oc}(t) = v_{bat,oc}(t_0) - \frac{1}{C_{bat}} \int_{t_0}^{t} i_{bat}(t)dt \quad\text{- (28)}$$

$$v_{bat}(t) = v_{bat,oc}(t) - R_{s,bat}i_{bat}(t)$$

$$i_{UC}(t) = i_{L2}(t)d_{S2} \quad\text{- (29)}$$

$$v_{UC,oc}(t) = v_{UC,oc}(t_0) \quad\text{- (30)}$$

$$-\frac{1}{C_{UC}} \int_{t_0}^{t} \left(i_{UC}(t) + \frac{v_{UC,oc}(t_0)}{R_{P,UC}} \right) dt \quad\text{- (31)}$$

$$v_{UC}(t) = v_{UC,oc}(t) - R_{S,UC}i_{UC}(t) \quad\text{- (32)}$$

In (27)-(32), current values of battery, UC, L_1, and L_2 represented by i_{bat}, i_{UC}, i_{L1}, and i_{iL2}, respectively. In addition, v_{bat} and v_{UC} are the terminal voltages of battery and UC while $v_{bat,oc}$ and $v_{UC,oc}$ are the open-circuit voltages of battery and UC. C_{bat} denotes the equivalent capacity of battery and $R_{s,bat}$ the equivalent serial resistance (ESR) of battery while C_{UC} denotes the normalized capacity of UC; in addition, $R_{S,UC}$ and $R_{P,UC}$ are the ESR and parallel resistance of UC, respectively. Fig. 5a. illustrates the simulation results of variations in input battery source during buck and Fig. 5b. boost operation mode while discharging.
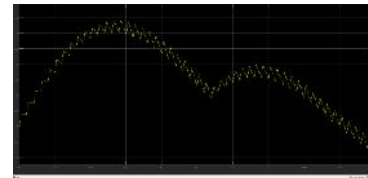

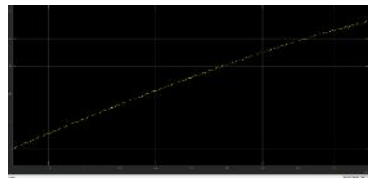Fig. 5a. Buck mode of operation while discharging

Fig. 5b. Boost mode of operation while discharging

Fig. 6a. illustrates the simulation results of variations in the output during buck and Fig. 6b. boost operation mode while discharging.
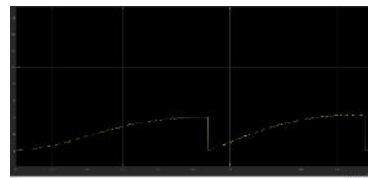
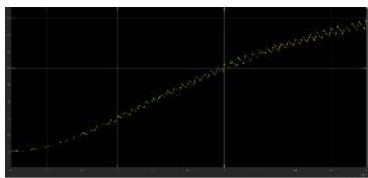

Fig. 6a. Buck mode of operation while discharging

Fig. 6b. Boost mode of operation while discharging

A prototype having maximum 255W output power is designed. In this prototype, the voltage and current values are measured by transducers and isolated gate drivers are utilized in order to provide isolation between the power and control levels; then the analog data related to these values is transmitted
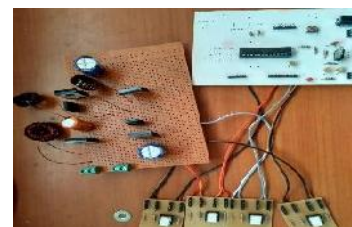

Fig. 7. Illustrates the proposed converter along with gate drivers

to the controller, DSPIC30F2010, via single strand wires. This kind of design not only provides a reliable and

robust control of the converter but also protects the microcontroller from possible threats. Table II gives the specifications of the prototype. Fig. 7. illustrates the prototype of proposed converter and Fig. 8. Illustrates motor/generator set.

Fig. 8. Motor-Generator Set

TABLE II

SPECIFICATIONS OF THE PROTOTYPE

Output voltage range	4 - 24V
Input voltage range	4 - 16V
Switching frequency	20KHz
Output capacitor	63V/100µF
Power switches	IRFP250N
Power diodes	MBR20200CT
Gate driver boards	TLP250
Battery	12V
UC	63V/2200µF

VI. CONCLUSION

This paper has successfully developed a novel SEPIC-based multi-input DC/DC converter. Based on the charging state of the ESS, two operation modes are defined. The steady-state and dynamic behavior of the proposed converter assessed the stability of the presented converter. Experimental results have been provided for two operation modes. The experimental results verified the analysis and feasibility of the proposed converter.

REFERENCES

[1] Alireza Khaligh, and Zhihao Li, "Battery, Ultracapacitor, Fuel Cell, and Hybrid Energy Storage Systems for Electric, Hybrid Electric, Fuel Cell, and Plug-In Hybrid Electric Vehicles: State of the Art," Vehicular Technology, IEEE Transactions on, vol. 59, no. 6, pp. 2806–2814, 2010.

[2] Mamadou Baïlo Camara, Hamid Gualous, Frederic Gustin, Alain Berthon, and Brayima Dakyo, "DC/DC Converter Design for Supercapacitor and Battery Power Management in Hybrid Vehicle Applications—Polynomial Control Strategy," Industrial Electronics, IEEE Transactions on, vol. 57, no. 2, pp. 587–597, 2010.

[3] Jian Cao, and Ali Emadi, "A New Battery/ UltraCapacitor Hybrid Energy Storage System for Electric, Hybrid, and Plug-In Hybrid Electric Vehicles," Power Electronics, IEEE Transactions on, vol. 27, no. 1, pp. 122-132, 2012.

[4] O. C. Onar, J. Kobayashi, and A. Khaligh, "A Fully-Directional Universal Power Electronic Interface for EV, HEV, and PHEV Applications," Power Electronics, IEEE Transactions on, vol. 29, no. 6, pp. 1–18, 2013.

[5] Furkan Akar and Bulent Vural, "Battery/UC Hybridization for Electric Vehicles via a Novel Double Input DC/DC Power Converter, "International Conference on Electric Power and Energy Conversion Systems, on, vol. 3, no. 1, pp. 296–307, 2013.

[6] Branislav Hredzak, Vassilios G. Agelidis, and Minsoo Jang, "A Model Predictive Control System for a Hybrid Battery-Ultracapacitor Power Source," Industrial Informatics, IEEE Transactions on, vol. 29, no. 3, pp. 1469–1479, 2014.

[7] Branislav Hredzak, Vassilios G. Agelidis, and Georgios D. Demetriades, "A Low Complexity Control System for a Hybrid DC Power Source Based on Ultracapacitor–Lead–Acid Battery Configuration," Energies, vol. 29, no. 6, pp. 2882–2891, 2014.

[8] Zhi-hui Ding, Chen Yang, Zhao Zhang, Cheng Wang, and Shao-jun Xie, "A Novel Soft-switching multi-Port Bidirectional DC-DC Converter for Hybrid Energy Storage System," Energy Conversion, IEEE Transactions on, vol. 23, no. 1, pp. 263–272, 2014.

[9] Junyi Shen, Serkan Dusmez, and Alireza Khaligh, "Optimization of Sizing and Battery Cycle Life in Battery/Ultracapacitor Hybrid Energy Storage Systems for Electric Vehicle Applications," Industrial Informatics, IEEE Transactions on, vol. 10, no. 4, pp. 2112– 2121, 2014.

[10] F. Akar, Y. Tavlasoglu, E. Ugur, B. Vural and I. Aksoy, "A Bidirectional Non-Isolated Multi- Input DC-DC Converter for Hybrid Energy Storage Systems in Electric Vehicles," Vehicular Technology, IEEE Transactions on, vol. 59, no. 6, pp. 2806–2814, 2015.

[11] Farouk Odeim, Jürgen Roes, and Angelika Heinzel, "Power Management Optimization of a Fuel Cell/ Battery/Supercapacitor Hybrid System for Transit Bus Applications," Vehicular Technology, IEEE Transactions on, vol. 27, no. 1, pp. 122–132, 2015.

.

[12] Furkan Akar, Yakup Tavlasoglu and Bulent Vural, "An Energy Management Strategy for a Concept Battery/Ultracapacitor Electric Vehicle with Improved Battery Life," Transportation Electrification, *IEEE Trānsactions on*, vol. 24, no. 3, pp. 862–868, 2016